Available online at www.sciencedirect.com
SCIENCE DIRECT
Journal of Catalysis 235 (2005) 69–78
JOURNAL OF CATALYSIS
www.elsevier.com/locate/jcat

Catalytic partial oxidation of ethanol over noble metal catalysts

J.R. Salge, G.A. Deluga, L.D. Schmidt *

Department of Chemical Engineering and Materials Science, University of Minnesota, 421 Washington Ave SE, Minneapolis, MN 55455, USA

Received 12 May 2005; revised 15 July 2005; accepted 20 July 2005

Available online 19 August 2005

Abstract

The catalytic partial oxidation of ethanol and ethanol-water was investigated over noble metal and metal plus ceria-coated alumina foams at catalyst contact times <10 ms. The effects of catalyst, flow rate, and water addition on selectivity and conversion were examined. Rh–Ce catalysts were the most active and stable. Without water addition, ethanol was converted directly to H_2 with >80% selectivity and >95% conversion with Rh–Ce catalysts. Rh, Pt, Pd, and Rh–Ru produced less H_2, with Pt and Pd producing <50% H_2. Pt, Pd, and Rh also produced more CH_4 and C_2H_4 than Rh–Ce. There was a smaller dependence on flow rate for Rh–Ce catalysts than other catalysts. Variation of a factor of 2 produced small changes in H_2, and lower flow rates produced less CH_4 and C_2H_4. Autothermal operation was achieved at as low as 10 mol% ethanol in water. Adding water to the Rh–Ce catalyzed reactor increased H_2 selectivity and reduced selectivity to CO to <50% due to increased water–gas shift and steam reforming activity. With added water, the selectivity to H_2 exceeds 100%, because both ethanol and water contribute H_2. Also, the total selectivity of all unwanted products, mostly CH_4, is <3% at the H_2 production maximum with water addition.

1. Introduction

Research in our laboratory over the past decade has focused on understanding partial oxidation reactions over noble metal catalysts at millisecond contact times. These partial oxidation systems can be run autothermally, thus eliminating the need for external heat. They can also be easily scaled up or down for different applications, enabling the use of a compact reactor suitable for stationary and portable applications. These autothermal reactor systems are also advantageous because they can be rapidly started up and can respond to process fluctuations at response times <5 s [1].

There have been numerous studies on hydrogen production by steam reforming of ethanol [2–6]. However, a major drawback to this approach is the fact that steam reforming is strongly endothermic,

$$C_2H_5OH + H_2O \rightarrow 2CO + 4H_2, \quad \Delta H^0 = +256\ \text{kJ/mol}. \tag{1}$$

Therefore, heat must be added to heat the reactor to the 800 °C needed to achieve high conversions, and this requires residence times of ∼1 s. Because external heat is required, reactor designs are typically limited by heat transfer rather than by reaction kinetics. There are ways to increase heat transfer while steam reforming fuels, such as in microchannel reactor systems [7] or catalytic wall reactors, where both endothermic and exothermic reactions take place on high-surface area catalysts [2]. However, the use of multiple fuels and expensive materials makes steam reforming unsuitable for transportation applications.

There has been discussion of the desirability of autothermal reforming of ethanol [8], and the catalytic partial oxidation and autothermal reforming of ethanol have been active areas of research [9–12]. Verykios et al. carried out their reactions by preheating ethanol to ∼500 °C over lanthanates, Ru, and Ni [10,11]. They accomplished their reactions at residence times ∼10 times longer than needed with millisecond contact time reactors. Cavallaro et al. carried out their reactions by preheating ethanol to ∼650 °C over Rh/Al_2O_3 powder [12]. Metal sintering was an issue in these experi-

* Corresponding author. Fax: +1-612-626-7246.
E-mail addresses: salge@cems.umn.edu (J.R. Salge), schmi001@umn.edu (L.D. Schmidt).

0021-9517/$ – see front matter
doi:10.1016/j.jcat.2005.07.021

ments, which were carried out in a furnace and focused on diluted ethanol solutions.

We recently reported that ethanol can be converted directly to H_2 with >80% selectivity and >95% conversion in an autothermal reformer using Rh–Ce catalysts [9]. Here we extend this research to examine the effects of catalyst and flow rate on the autothermal reforming of ethanol at catalyst contact times <10 ms. Noble metals (Rh, Pt, and Pd), noble metal alloys (Rh–Ru), and the addition of ceria (Rh–Ce) are examined. The effect of flow rate is also investigated.

Unlike hydrocarbons, the partial oxidation of ethanol is slightly endothermic, so it alone will not produce the heat necessary for autothermal operation:

$$C_2H_5OH + (1/2)O_2 \rightarrow 2CO + 3H_2, \quad \Delta H^0 = +14\,\text{kJ/mol}. \tag{2}$$

Thus some total oxidation is needed to generate the heat for operation at the 700–1200 °C necessary for sustained fast reaction:

$$C_2H_5OH + 3O_2 \rightarrow 2CO_2 + 3H_2O, \quad \Delta H^0 = -1277\,\text{kJ/mol}. \tag{3}$$

Although the combustion reaction is highly exothermic, it can also produce flames. Flames are intolerable because they lead to unsteady operation and form coke and soot, which deactivate the catalyst. Homogeneous reactions also form unwanted products, such as acetaldehyde and ethylene [13].

To generate more hydrogen, the steam reforming and partial oxidation reactions can be combined with the water–gas shift (WGS) reaction:

$$CO + H_2O \rightarrow CO_2 + H_2, \quad \Delta H^0 = -41\,\text{kJ/mol}. \tag{4}$$

Along with generating more H_2, the WGS reaction is important because it reduces the CO concentration, and CO is a poison to PEM fuel cells. The exothermic WGS reaction generally goes to equilibrium at the high temperatures required for the reforming reactions, but it requires low temperatures for favorable H_2 equilibrium, at which point it becomes kinetically limited [14].

By combining oxidation with steam reforming and WGS, one can take advantage of the heat generated by total oxidation and the extra H_2 produced by steam reforming and WGS. Stoichiometrically, these three reactions can be written as

$$C_2H_5OH + 2H_2O + (1/2)O_2 \rightarrow 2CO_2 + 5H_2, \quad \Delta H^0 = -68\,\text{kJ/mol}. \tag{5}$$

Thus adding water with air should maximize hydrogen production and minimize CO in an exothermic process. Ethanol–water mixtures are also beneficial because the need to remove all the water is a significant cost in producing fuel grade ethanol. Fermentation produces 10–20 moles of water per moles of ethanol. Distillation and water separation from the azeotrope using zeolite adsorption are then necessary to produce fuel-grade ethanol.

2. Experimental

2.1. Reactor

Ethanol–air mixtures are flammable over a wide composition range [15]. To avoid the formation of flames and to help limit other homogeneous reactions before the catalyst, we used an automotive fuel injector [16], which can deliver and vaporize fuel rapidly by creating small droplets. Because vaporization and mixing of the fuel with air occur almost simultaneously, upstream regions containing a combustible mixture are reduced or avoided.

The reactor was identical to that described previously and consists of a quartz tube, 50-cm long with an 18-mm i.d. [9]. The fuel (ethanol or ethanol–water mixture), which is liquid at room temperature, was introduced at the top of the reactor using a fuel injector. Pressurized fuel at 20 psig fed the injector, controlled using LabVIEW at frequencies of 10–20 Hz and at duty cycles (i.e., the percentage of time that the injector remains open) of 3–15%. The liquid flow rate delivered by the injector was accurately controlled by the pressure in the fuel supply tank and by the duty cycle. The fuel delivery rate was calibrated at different frequencies and duty cycles and was accurate to within ±2%. In all experiments, the reactor ran at atmospheric pressure.

The fuel injector accurately dispersed the fuel into a 25-cm-long preheated section of the reactor. Preheating of 140 ± 10 °C was maintained above the catalyst using heating tape wrapped around this preheat section. Oxygen and nitrogen were mixed at air stoichiometry ($N_2/O_2 = 3.76$) and then introduced at the beginning of the preheat section. The flow rates of high purity oxygen and nitrogen entering the system from high-pressure cylinders were adjusted using mass flow controllers via LabVIEW; these controllers are accurate to within ±5% of their setpoint. Mixing of the air and fuel was improved by adding a blank ceramic foam at the end of the preheat section, about 4 cm above the catalyst.

The catalyst-coated foam had uncoated foams placed upstream and downstream to prevent axial heat loss by radiation. The upstream heat shield also promoted additional radial mixing of the reactants. The foams were sealed in the quartz tube using an alumina-silicate cloth gasket that prevents bypassing of gases. A hole was bored along the axis of the downstream heat shield so that a chromel–alumel k-type thermocouple could touch the back face of the catalyst in the same location for each experiment. Alumina–silica insulation was placed around the outside of the reactor to minimize radial heat losses. A sample of the products was obtained for analysis at the reactor outlet using a gas-tight syringe.

2.2. Catalyst preparation

Ceramic foams (92% Al_2O_3, 8% SiO_2) were used as catalyst supports. They were supplied at 80 pores per linear inch (ppi) in cylindrical segments 10 mm long and 17 mm in diameter. The foams have a nominal surface area ∼1.0 m^2/g,

an average channel diameter of ∼200 μm, and a void fraction of ∼80%. These foams were coated by the wet impregnation method as described previously [17].

For single metal catalysts (Rh, Pt, and Pd), the metals were coated on the supports by soaking them in an aqueous solution of the corresponding metal precursor salt ($Rh(NO_3)_3$, H_2PtCl_6, or $PdCl_3$). The foams were dried and calcined at 600 °C for 6 h. A calculated amount of metal salt was used to ensure ∼5 wt% metal loading based on the mass of the foam.

A γ-Al_2O_3 washcoat was added to select Rh catalysts to decrease channel size and increase surface area [17]. The supports were washcoated using a 3 wt% γ-Al_2O_3 slurry in water, followed by drying and heating at 600 °C for 6 h in a closed furnace. Typical washcoats were ∼5% by weight of the foam, for which an average alumina film thickness of 10 μm was measured by scanning electron microscope analysis. After the washcoat was applied, the foam was coated with Rh as described previously.

The Rh–Ru catalysts were prepared by dipping the foams in an aqueous mixture of $Rh(NO_3)_3$ and 0.1 mol $K_2RuCl_5(H_2O)$ in 1.0 mol H_2SO_4. A calculated amount of solution was used to ensure a metal loading of ∼2.5 wt% each of Rh and Ru. The catalysts were dried and calcined at 600 °C for 6 h.

For the catalysts combining Rh with ceria, a calculated amount of $Rh(NO_3)_3$ and $Ce(NO_3)_3{\cdot}6H_2O$ that when deposited on the support would lead to ∼2.5 wt% each of Rh and ceria were mixed together in an aqueous solution. The foam was soaked in this solution, dried, and then calcined at 600 °C for 6 h.

All experiments were run for up to 30 h on a given catalyst, and most experiments were repeated on several nominally identical catalyst samples with no systematic differences or deactivation noted.

2.3. Product analysis

Once the back-face temperature of the catalyst had stabilized (⩽10 min), a sample of the product gases was obtained through a septum at the exit of the reactor. A gas-tight syringe was used to withdraw product samples and inject them into a dual-column gas chromatograph equipped with thermal conductivity and flame ionization detectors. Column retention times and response factors were determined by injecting known species. Because nitrogen is an inert species, it was used as the calibration gas for mass balances. Mass balances on carbon and hydrogen typically closed to within ±5%.

Product selectivities were calculated on an atomic basis. Both C and H atom selectivities were calculated as the ratio of the moles of a specific product to the total moles of all products, accounting for stoichiometry. The three H_2 molecules from C_2H_5OH represent 100% H_2 selectivity. Thus, if pure ethanol is fed to the system, then maximum H_2 selectivity is 100%; however, if an ethanol–water mixture is injected into the system, then H_2 selectivity can exceed 100%. This is possible if water is consumed in the process, because the H atoms from the H_2O can also be converted into H_2. According to the reaction of interest (Eq. (5)), complete conversion of the ethanol and water could generate 5 H_2 per C_2H_5OH, which gives a maximum H_2 selectivity of 5/3, or 167%. The consumption of added water results in negative selectivity to H_2O, but total H atom selectivity still sums to unity.

3. Results

In these experiments the C/O ratio was varied at a constant total flow rate. The C/O ratio for ethanol and ethanol–water mixtures is defined as the amount of C atoms entering the reactor with ethanol divided by the number of O atoms entering with oxygen and ethanol. Therefore, a C/O ratio of 2.0 corresponds to pure ethanol, a ratio of 1.0 corresponds to syngas (H_2 and CO) stoichiometry according to Eq. (2), and a ratio of 0.29 corresponds to combustion according to Eq. (3). The lowest C/O ratios shown represent the point at which experiments were halted because of pulsing in the catalyst, where compositions were within the flammability regime of ethanol–air mixtures. The maximum C/O ratios shown are the highest ratios that could be maintained in autothermal operation without the catalyst extinguishing due to a fuel-rich mixture.

3.1. Effect of catalyst

We investigated several noble metal and metal plus ceria-coated alumina foams. The single metal catalysts (Rh, Pt, and Pd) were ∼5 wt% of the metal based on the total mass of the foam. A γ-Al_2O_3 washcoat was added to select Rh catalysts (denoted as Rh wc in Fig. 1) to decrease the channel size and increase the surface area of the catalyst, which has been found to increase syngas selectivity and reduce olefins [17]. The addition of ceria to noble metal catalysts has been shown to increase WGS activity [18] and is also commonly used as an oxygen donor for automotive catalytic converters [19]. Therefore, foams were loaded with ∼2.5 wt% each of Rh and Ce. The catalytic partial oxidation of ethanol over structured Ru catalysts has been shown to produce high selectivity to syngas, although these experiments were conducted in a furnace and at longer contact times [10]. Here Rh and Ru were combined with ∼2.5 wt% each based on the mass of the foam.

The effect of the catalyst on reactor temperature, conversion, and selectivity for the reforming of ethanol is shown in Fig. 1. The total flow rate for these experiments was 6 slpm, resulting in a calculated catalyst contact time of ∼7 ms at 700 °C. The corresponding gas hourly space velocity (GHSV) was $\sim 1.5 \times 10^5\ h^{-1}$. Ethanol conversion was >85% and oxygen conversion (not shown) was >99% for all ratios and catalysts considered. Pt and Pd had a higher back-face temperature, while the other catalysts operated within a

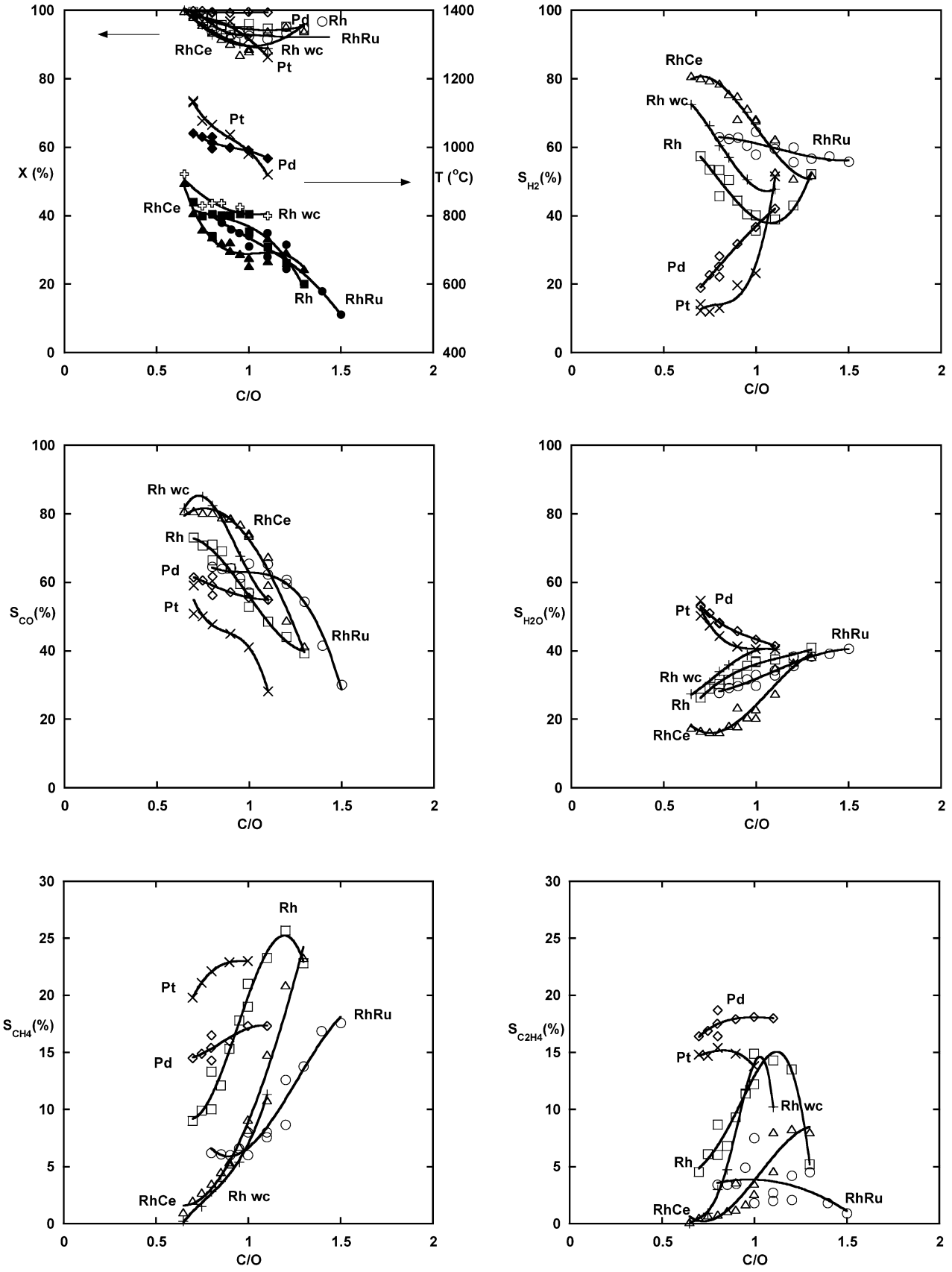

Fig. 1. Comparison of the reforming of ethanol over Rh, Rh–Ce, Rh–Ru, Pt, and Pd coated foams at a total flow rate of 6 SLPM. Ethanol conversion (X), catalyst back-face temperature (T), and product selectivities are shown as a function of C/O ratio.

similar temperature range, about 200 °C cooler. As the feed becomes more fuel-rich, the back-face temperature of all of the catalysts decreases, as expected. As shown in Fig. 1, the order of effectiveness in syngas production is Rh–Ce >Rh–wc >Rh–Ru >Rh >Pd >Pt. Rh–Ce is more stable and gives greater WGS activity than noble metals alone. The selectivity to H_2 peaks at ∼80% at a C/O ∼0.7 for Rh–Ce. Rh, Pt, Pd, and Rh–Ru produced less H_2, with Pt and Pd producing <50% H_2. The range of operation of Pt and Pd was also limited. Pt was difficult to ignite and was unstable at low C/O ratios, and Pd showed immediate coke formation, eventually causing extinction in the reactor. Rh–Ru showed ∼65% selectivity to H_2; however, it was difficult to maintain steady state at lower C/O ratios.

The minor products observed consisted of CH_4, C_2H_4, CH_3CHO, and C_2H_6. At low C/O ratios, the production of minor products was <3% for Rh–Ce. Meanwhile, Pt and Pd produced ∼15% each of CH_4 and C_2H_4. Only small amounts of CH_3CHO and C_2H_6 (not shown) were produced on any of the catalysts at low C/O ratios. CH_3CHO was produced by ethanol dehydrogenation and was completely reformed at high temperatures (low C/O ratios). As the fuel in the feed increased, more CH_3CHO was produced.

For the experimental conditions investigated, the major products predicted by thermodynamic equilibrium are H_2, H_2O, CO, CO_2, and CH_4. The selectivity to CH_4 is high at low temperatures (>50%), but decreases rapidly above 500 °C and becomes negligible above 800 °C. This decrease in CH_4 is accompanied by a corresponding increase in H_2 selectivity. At low C/O ratios, product selectivities from reforming ethanol over Rh–Ce coated foams were within ±3% of those predicted by thermodynamic equilibrium. At a C/O ∼ 0.7, the Rh–Ce catalyst back-face temperature was ∼810 °C. At this temperature, equilibrium predicts a H_2 selectivity of 82.9% and a H_2O selectivity of 16.9%. Selectivities to CO, CO_2, and CH_4 are 82.0, 17.9, and <0.2%, respectively. Only negligible amounts of CH_3CHO, C_2H_4, and C_2H_6 are predicted.

3.2. Effect of flow rate

The effect of flow rate on the reforming of ethanol was studied over Rh and Rh–Ce catalysts. For these experiments, the total flow rate was varied from 8, 6, and 4 slpm (GHSV ∼ 2, 1.5, and 1×10^5 h^{-1}). These correspond to catalyst contact times of 5–10 ms at 700 °C. Oxygen conversion was >99% for all ratios and flow rates considered.

Fig. 2 shows the effect of flow rate on the reformation of ethanol over Rh catalysts. Ethanol conversion was >95% for all flow rates, whereas the back-face temperature of the catalyst increased slightly with increasing flow rate. This increase in temperature was more apparent at lower C/O ratios. Reducing the total flow rate increased the syngas selectivity and decreased higher products. Selectivity to H_2 reached a maximum of ∼75% at a flow rate of 4 slpm, but was reduced to <50% at 8 slpm. More minor products were produced at higher flow rates. Selectivity to CH_4 and C_2H_4 both increased sharply with higher flow rates, and their selectivity peaked at C/O ∼ 1.1 for all flow rates. Meanwhile, selectivity to C_2H_6 and CH_3CHO (not shown) were independent of flow rate, but increased with increasing C/O ratio.

The Rh–Ce catalysts had a less pronounced dependence on flow rate. Fig. 3 shows the dependence of temperature, conversion and product selectivities on flow rate for Rh–Ce catalysts. Ethanol conversion was >95% for all flow rates. The catalyst back-face temperature increased with increasing flow rate because at higher flow rates the rate of heat generation increases, causing the reactor to operate closer to adiabatic.

Selectivities to syngas (H_2 and CO) and combustion products (CO_2 and H_2O) depended only slightly on flow rate. Over this range of flow, selectivity to H_2 varied by ∼10% at a given C/O ratio, whereas selectivity to CO and combustion products exhibited a smaller variation. As was the case with Rh catalysts, more CH_4 and C_2H_4 were produced at higher flow rates, whereas CH_3CHO and C_2H_6 production (not shown) remained relatively constant. Production of all the minor products increased as the feed became more fuel-rich for all flow rates.

3.3. Water addition

Because Rh–Ce is more stable and gives greater WGS activity, it was used as the catalyst for water addition experiments. Typical results for the reforming of ethanol over Rh–Ce with added water are shown in Fig. 4. These experiments were done at a constant total flow rate of 6 slpm, resulting in a calculated catalyst contact time of ∼7 ms at 700 °C. Curves are shown for pure ethanol (100%) and ethanol–water mixtures of 75, 50, 25, 20, and 10% ethanol by mole. On a weight basis, 10 mol% ethanol corresponds to 22 wt% ethanol, or 53 “proof.” This is close to the upper limit of ethanol from fermentation.

For pure ethanol and ethanol–water mixtures, ethanol conversion remained >95% for all C/O compositions. Adding water increased the selectivity to H_2. For pure ethanol, the selectivity to H_2 peaked at ∼80% at C/O ∼ 0.7, whereas for 10% ethanol, the selectivity to H_2 exceeded 100%, because both ethanol and water contribute H_2. Meanwhile, the selectivity to CO decreased with added water, due to increased WGS and steam reforming activity. For pure ethanol, selectivity to CO peaked at ∼80% at C/O ∼ 0.7, whereas for 10% ethanol, the selectivity to CO was <50%. Thus, the H_2/CO ratio rose to 6.3/1 and the CO/CO_2 ratio fell to 1/2.3 for 10% ethanol.

As expected, the minor products were CH_4, C_2H_4, C_2H_6, and CH_3CHO, and the total of these products was <3% at the H_2 maximum of C/O ∼ 0.7, rising as C/O increased. CH_4 is the major byproduct of pure ethanol and ethanol–water mixtures. Selectivity to CH_4 rose quickly with increasing C/O ratio. Adding up to 50% water changed the selectivity to CH_4 only slightly. However, at ethanol com-

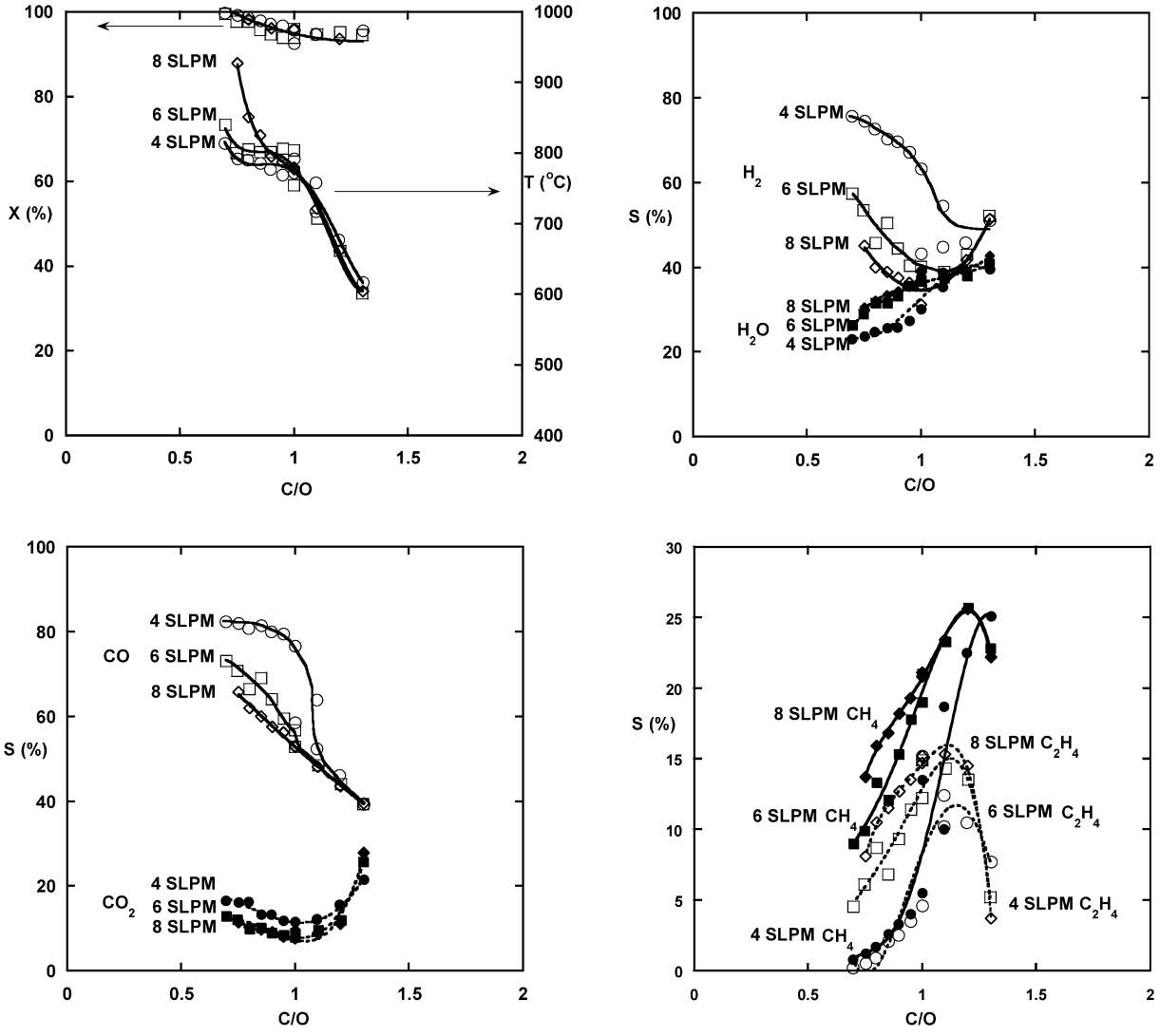

Fig. 2. The effect of flow rate on the reforming of ethanol over Rh at 8, 6, and 4 SLPM, which corresponds to catalyst contact times of 5 to 10 ms. Ethanol conversion (X), catalyst back-face temperature (T), and product selectivities are shown as a function of C/O ratio.

positions <25% ethanol, more CH_4 is produced due to decreased catalyst temperature. Methane is undesirable in this process because it competes with H_2 for hydrogen atoms, but is inert in PEM fuel cells.

Unlike CH_4, selectivity to C_2H_4 and C_2H_6 (results not shown) decreased when water was added. For pure ethanol and ethanol–water mixtures, C_2H_4 formation peaked at a C/O ∼ 1.1 and then quickly declined. A negligible amount of C_2H_6 was formed for ethanol–water mixtures with <50% ethanol. The selectivity to CH_3CHO (results not shown) had no clear dependence on water addition.

3.4. Blank experiment

To further study the effectiveness of producing syngas on these catalysts, experiments were carried out in which an uncoated alumina foam was inserted into a quartz tube and placed in a furnace. The fuel was vaporized and mixed with air at a C/O ∼ 1.0, then introduced to the furnace, which was heated between 250 and 900 °C. Ethanol and air were introduced at a total flow rate of 6 slpm, which corresponds to residence times of the gases in the furnace of 200–400 ms. Ethanol conversion remained >90% and oxygen conversion was >99%, which are feasible because ethanol can decompose completely at high temperatures even in the absence of a catalyst [3]. However, the selectivity to H_2 fell to ∼25%, and carbon formation on the blank foam was observed. Selectivity to CH_4 and C_2H_4 rose with temperature to ∼25 and ∼20% at 900 °C, respectively. Production of CH_3CHO fell as the temperature increased, but was still ∼5% at 900 °C.

3.5. Homogeneous modeling

An elementary reaction mechanism to describe high-temperature ethanol oxidation has been proposed by Marinov [13]. This comprehensive model incorporates 57 species and more than 370 elementary reactions. Note that this model has not been validated within our operating range.

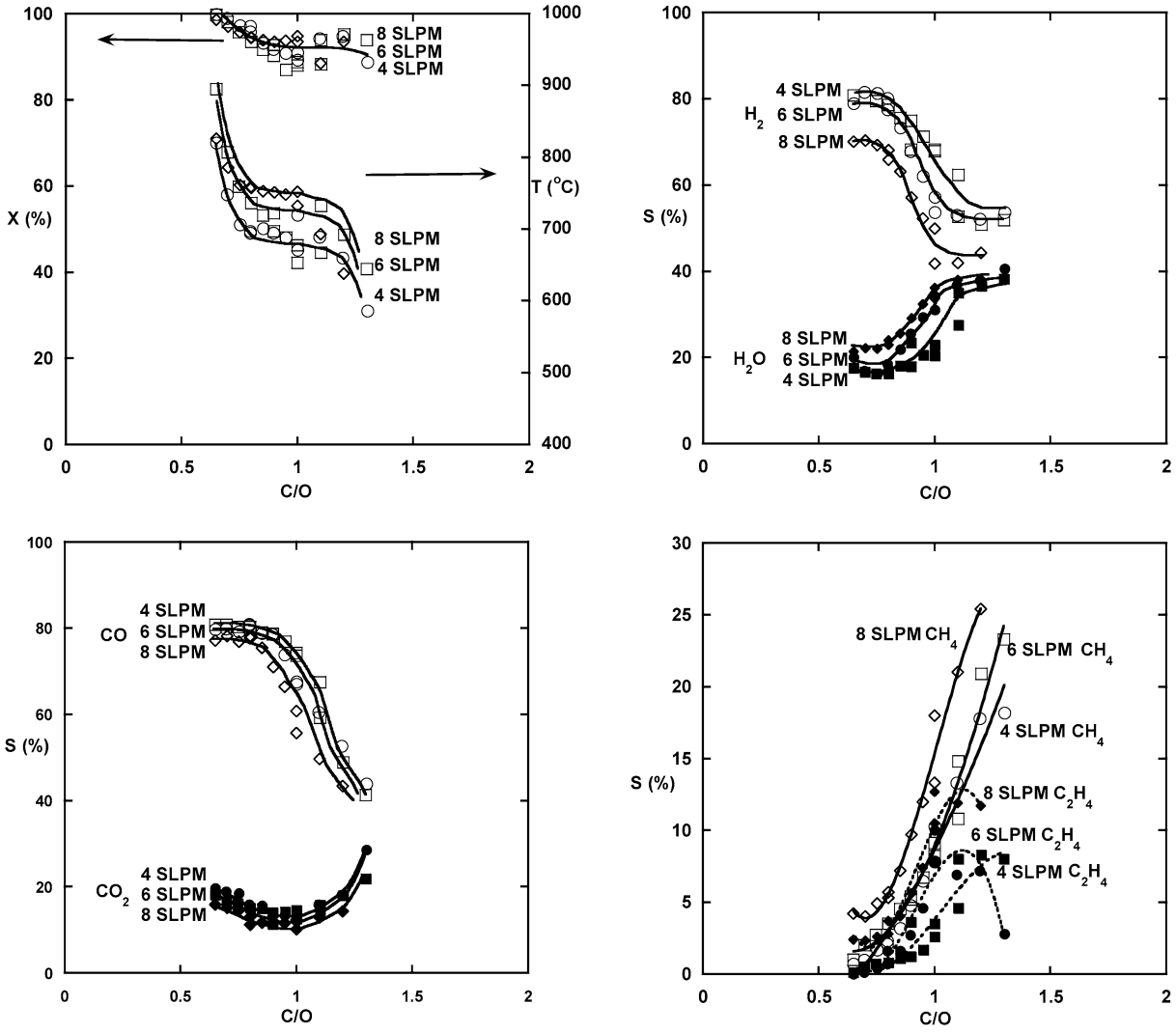

Fig. 3. The effect of flow rate on reforming of ethanol over Rh–Ce at 8, 6, and 4 SLPM, which corresponds to catalyst contact times of 5 to 10 ms. Ethanol conversion (X), catalyst back-face temperature (T), and product selectivities are shown as a function of C/O ratio.

Using ChemKin, the Marinov model was solved assuming a plug flow reactor with an isothermal temperature profile. A similar approach was used by Hudgins et al., who compared the Marinov model to empty tube experiments in a temperature range of 600–800 °C, a residence time of 4 s, and a C/O of 1.0 [20]. These authors found that the Marinov model predicts trends, but does not reproduce the experimental data accurately. They attributed this difference to experimental error in recording temperatures. Our results in the present work show better agreement between the model and our blank tube experiments.

The Marinov model was used to predict conversions and product selectivities at our experimental conditions. Results obtained over Rh–Ce are compared with those predicted from homogeneous chemistry using the Marinov model in Fig. 5. A total flow rate of 6 slpm was used for both. The model assumes a constant temperature of 900 °C and a residence time of 200 ms, which is greater than the catalyst contact time of <10 ms in these experiments. Complete conversion of ethanol and oxygen (data not shown) at these conditions was predicted. The presence of the Rh–Ce catalyst dramatically increased syngas selectivity. Production of H_2 increased by a factor of 4 at C/O ∼ 0.7, whereas selectivity to CO increased by ∼20%. The model predicts that CH_4 selectivity will be fairly constant at ∼20%, whereas over Rh–Ce, <3% was observed at a C/O ∼ 0.7, but it increased with C/O to ∼20%. Selectivity of C_2H_4 over Rh–Ce was <1% at C/O ∼ 0.7 and increased to only ∼10% at higher C/O. However, the model predicts ∼10% at the low C/O and >35% at the higher C/O. Analysis of this mechanism identifies the primary oxidation pathway proceeding through CH_3CHO. However, the model predicts that CH_3CHO will be completely reformed to CO and CH_4 at the conditions chosen here.

The predicted selectivities from the homogeneous model at C/O ∼ 1.0 are comparable to those from the blank experiment at 900 °C, shown to the right in Fig. 5. The residence time of the gases for both was ∼200 ms. The model pre-

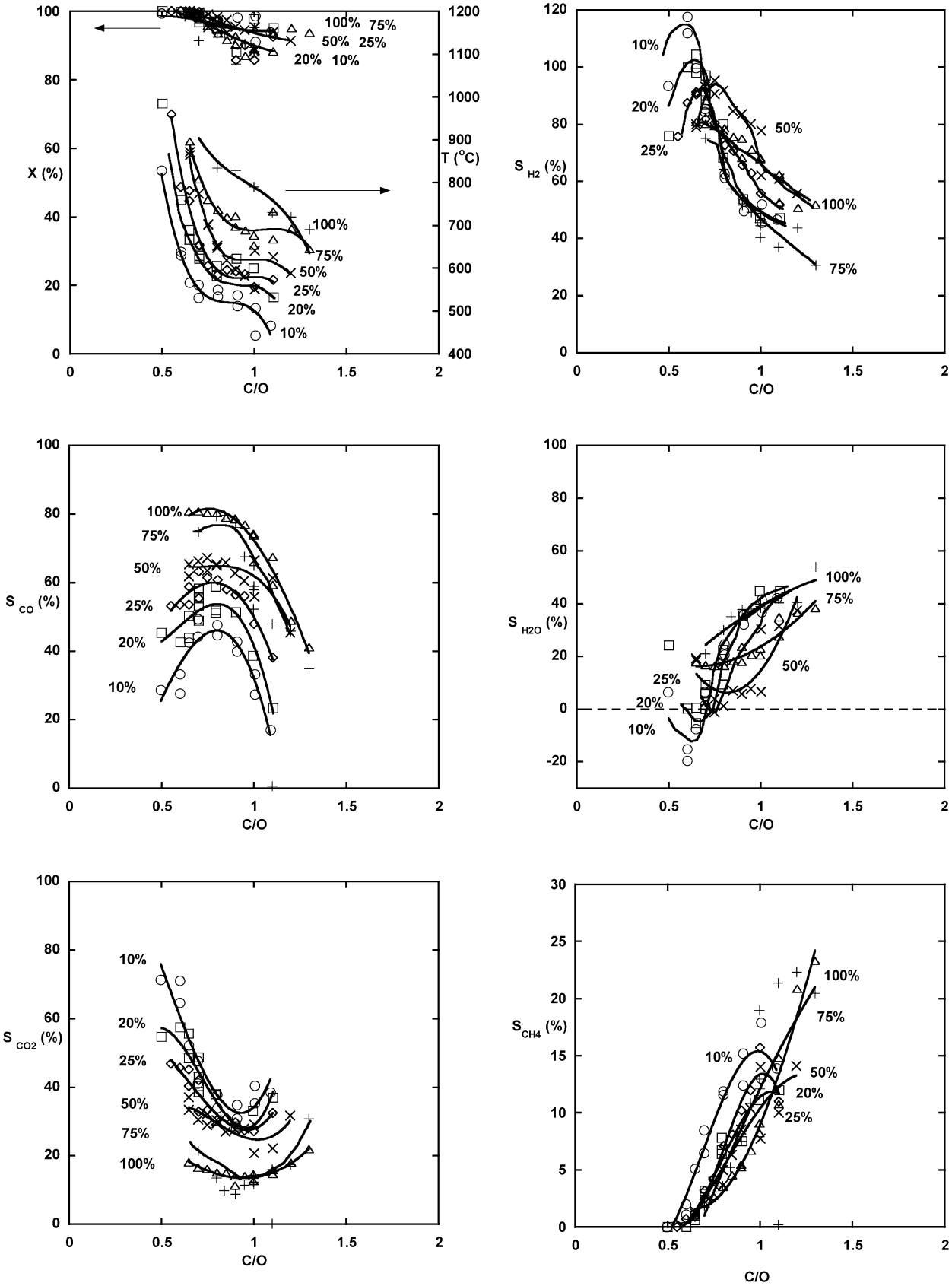

Fig. 4. The effect of water on the reforming of ethanol over Rh–Ce at 6 SLPM. Curves are shown for pure ethanol (100%) and ethanol–water mixtures of 75, 50, 25, 20, and 10% ethanol on a mole basis. Ethanol conversion (X), catalyst back-face temperature (T), and product selectivities are shown as a function of C/O ratio.

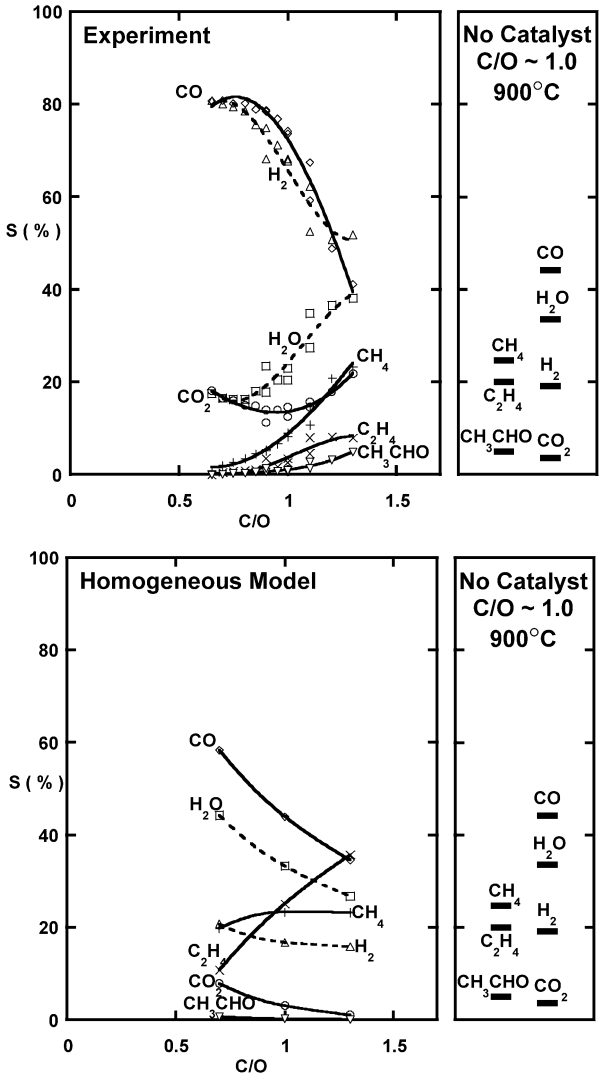

Fig. 5. Product selectivities observed experimentally over Rh–Ce and those predicted using a homogeneous model are shown on the left as a function of C/O ratio. On the right are product selectivities observed in the blank experiment at C/O ∼ 1.0 and 900 °C. The total flow rate was 6 SLPM and the model assumes a constant temperature of 900 °C and a residence time of 200 ms.

dicts H_2, H_2O, CO, CO_2, and CH_4 selectivities to within 2%. However, the model overpredicts C_2H_4 selectivity and underpredicts CH_3CHO selectivity by ∼5%.

4. Discussion

4.1. Surface reactions

Ethanol adsorption and decomposition have been carefully examined on well-defined single crystal surfaces. Ethanol adsorbs dissociately via scission of the O–H bond as an ethoxide species [21–23]. Over Pt and Pd, ethoxides are subsequently dehydrogenated to acetaldehyde [23]. However, over Rh, ethoxides do not yield acetaldehyde [21], but rather dehydrogenate via β-CH scission to form an oxametallacycle, which decomposes to adsorbed carbon, hydrogen, and oxygen species. These species then recombine to form the syngas products observed in the present study. Surface reactions forming products more complex than C_1 carbon species do not exist [18]. Most other species are probably formed by homogeneous reactions.

Ethanol and acetaldehyde do not decarbonylate via a common pathway on Rh. Once acetaldehyde is formed, it adsorbs as η^2-acetaldehyde, with the α-carbon and the oxygen bonded to the metal. This is followed by C–C bond scission to form CO and methyl, then methane [21]. This could explain the high methane selectivity observed at high C/O.

4.2. Gas phase reactions

Under the conditions used here, all reactions appear to occur on the surface, except for the formation of minor products such as acetaldehyde and ethylene. Analysis of the Marinov mechanism identifies the primary ethanol oxidation pathway proceeding through acetaldehyde [13]. The α-CH bonds are the weakest in ethanol, and the model predicts that abstraction of one of these produces acetaldehyde and H atoms. This explains why acetaldehyde was observed with ethanol, when previous work on the partial oxidation of alkanes over noble metal coated foams produced no oxygenates [24].

Selectivities were predicted using the homogeneous gas phase mechanism. As shown in Fig. 5, much more CH_4 and C_2H_4 would have been formed had gas phase chemistry dominated. It has been observed in this laboratory that with alkanes, syngas is seen at low C/O and olefins are seen at higher C/O. However, with ethanol, olefin production never increased above ∼10%, even at the highest C/O before autothermal operation extinguished.

4.3. Effect of catalyst

The choice of catalyst is a crucial factor in determining syngas yield. Rh–Ce was the most stable and gave greater syngas selectivity than noble metals alone. This is perhaps because Ce was able to store oxygen and make it available for reaction via a redox reaction [18]. Ru cannot undergo this redox reaction, so the addition of Ru to Rh did not increase syngas yield as did the addition of Ce. Pt and Pd produce less syngas than the Rh-containing catalysts. They run at a higher back-face temperature, which can in turn generate more products of homogeneous chemistry. The increase in higher products on these catalysts led to coking, which caused the Pd catalyst to extinguish.

4.4. Effect of washcoat

Application of a γ-Al_2O_3 washcoat to Rh catalysts has been found to decrease channel size and increase surface area of the catalyst [17]. Because Rh promotes syngas production, the increased surface area of Rh due to washcoating

was found to improve syngas yields for the partial oxidation of alkanes. This work shows that adding a washcoat to Rh catalyst increases syngas selectivity ∼10%. However, Rh–Ce is still a superior producer of syngas.

4.5. Rh stability

After 4–6 h of operation, the Rh catalyst was no longer stable, and it began to deteriorate and crumble. There was no noticeable change in the operation of the reactor or in product yields, but when the reactor was dismantled, it was found that the Rh-coated foam had turned to powder. The addition of a washcoat to the Rh catalyst produced the same result. However, this behavior was not observed for Rh–Ce, Rh–Ru, Pt, or Pd.

Deterioration of a Rh/Al_2O_3 catalyst is not unique to this system. Cavallaro et al. noticed that when oxygen is added during the steam reforming of ethanol, Rh crystallites sinter [12]. They hypothesized that this was due to strong local temperature increases (hot spots) produced by the total oxidation of ethanol. Their experiments were done using powder catalyst, so they did not observe the destruction of the foam. The reason for the deterioration of Rh/Al_2O_3 catalysts during the autothermal reforming of ethanol is currently under investigation.

5. Conclusions

High selectivities to H_2 were achieved from the catalytic partial oxidation of ethanol and ethanol–water. Short-contact time reactors can be tuned by changing catalyst, flow, and feed conditions. Rh–Ce catalysts gave the highest selectivity to syngas and were the most stable, perhaps due to the redox capabilities of Ce. Less H_2 and more minor products were produced over Rh, Rh–Ru, Pt, and Pd catalysts. The addition of washcoat to Rh increased syngas selectivity, but had no effect on stability. Flow variation by a factor of 2 produced only small changes in H_2 production for Rh–Ce compared with other catalysts.

Autothermal operation was achieved down to 10 mol% ethanol in water. The addition of water to the Rh–Ce catalyzed reactor increased H_2 selectivity to $>100\%$, because both ethanol and water contribute H_2. Due to increased WGS and steam reforming activity, CO selectivity decreased to $<50\%$ with added water. At the H_2 production maximum, total selectivity to unwanted products was $<3\%$ with water addition.

Under the conditions used in these experiments, surface reactions dominated. Ethanol adsorbed dissociately as an ethoxide species and then decomposed to carbon, oxygen, and hydrogen species. These then reacted rapidly on the surface to form H_2 and CO; no reaction pathways on the surface to form greater than C_1 products were found to exist. If homogeneous reactions had dominated, then less syngas and much more CH_4 and C_2H_4 would have been observed.

Acknowledgments

This research was partially supported by grants from the Minnesota Corn Growers Association and the Initiative for Renewable Energy and the Environment at the University of Minnesota.

References

[1] C.A. Leclerc, J.M. Redenius, L.D. Schmidt, Catal. Lett. 79 (2002) 39.
[2] E.C. Wanat, K. Venkataraman, L.D. Schmidt, Appl. Catal. A 276 (2004) 155.
[3] A.N. Fatsikostas, D.I. Kondarides, X.E. Verykios, Chem. Commun. 2001 (2001) 851.
[4] A.N. Fatsikostas, D.I. Kondarides, X.E. Verykios, Catal. Today 75 (2003) 145.
[5] D.K. Liguras, D.I. Kondarides, X.E. Verykios, Appl. Catal. B 43 (2003) 345.
[6] S. Cavallaro, Energy Fuels 14 (2000) 1195.
[7] A.Y. Tonkovich, S. Perry, Y. Wang, D. Qui, T. LaPlante, W.A. Rogers, Chem. Eng. Sci. 59 (2004) 4819.
[8] L.F. Brown, Int. J. Hydrogen Energy 26 (2001) 381.
[9] G.A. Deluga, J.R. Salge, L.D. Schmidt, Science 303 (2004) 993.
[10] D.K. Liguaras, K. Goundani, X.E. Verykios, Int. J. Hydrogen Energy 29 (2004) 419.
[11] D.K. Liguaras, K. Goundani, X.E. Verykios, J. Power Sources 130 (2004) 30.
[12] S. Cavallaro, V. Chiodo, A. Vita, S. Freni, J. Power Sources 123 (2003) 10.
[13] N.M. Marinov, Int. J. Chem. Kinet. 31 (1999) 183.
[14] T. Bunluesin, R.J. Gorte, G.W. Graham, Appl. Catal. B 15 (1998) 107.
[15] B. Lewis, G. von Elbe, Combustion, Flames and Explosions of Gases, Academic Press, New York, 1987, p. 706.
[16] J.J. Krummenacher, K.N. West, L.D. Schmidt, J. Catal. 215 (2003) 332.
[17] A.S. Bodke, S.S. Bharadwaj, L.D. Schmidt, J. Catal. 179 (1998) 138.
[18] C. Wheeler, A. Jhalani, E.J. Klein, S. Tummala, L.D. Schmidt, J. Catal. 223 (2004) 191.
[19] K.C. Taylor, in: J.R. Anderson, M. Boudart (Eds.), Automobile Catalytic Converters, Catalysis: Science and Technology, vol. 5, Springer, Berlin, 1984.
[20] D.O. Christensen, P.L. Silveston, E. Croiset, R.R. Hudgins, Ind. Eng. Chem. Res. 43 (2004) 2636.
[21] C.J. Houtman, M.A. Barteau, J. Catal. 130 (1991) 528.
[22] M. Mavrikakis, M.A. Barteau, J. Mol. Catal. A: Chem. 131 (1998) 135.
[23] A. Yee, S.J. Morrison, H. Idriss, Catal. Today 63 (2000) 327.
[24] M. Huff, P.M. Torniainen, L.D. Schmidt, Catal. Today 21 (1994) 113.